Time resolved and site selective spectroscopy of thulium doped into germano- and alumino-silicate optical fibres and preforms

J.R. Lincoln [a], W.S. Brocklesby [a], F. Cusso [b,1], J.E. Townsend [b], A.C. Tropper [b] and A. Pearson [a]

[a] Department of Physics and [b] Optoelectronics Research Centre, University of Southampton, Southampton, SO9 5NH, UK

Optical properties of thulium ions doped in varying concentrations into germano- and alumino-silicate glass fibres and their preforms are studied. Absorption and fluorescence spectra are shown to vary little with thulium concentrations up to 12000 ppm, but vary drastically with germanium or aluminium codopant. Resonant fluorescence studies of Tm^{3+} show correlations in the movements of the Stark levels of the ground state, indicating systematic correlations between the ion site and Stark level position. An upper limit of 10 cm^{-1} for the homogeneous line width of thulium in alumino-silicate glass is established at 9 K. The lifetimes of the $^1G_4$ and $^3F_4$ levels are studied and are related to codopant influence and cross-relaxation which are linked to fibre drawing and Tm^{3+} concentration. A significant lifetime shortening is observed on drawing preform to fibre. A model is presented for non-exponential decay of the $^3F_4$ level. Three- and four-level rate equations have been successfully used to simulate the observed rise of the $^3F_4$ fluorescence and decay of the $^1D_2$ fluorescence, excited resonantly and by up-conversion processes, respectively. These models yield both the excitation pump rate and cross-relaxation rates.

1. Introduction

The simple glass network which forms the core region of a germano-silicate communications-type fibre is an interesting host medium in which to study spectroscopic properties of lanthanide dopant ions. The immediate environment of such an ion and the degree to which it disrupts the glass network remain unknown. In laser glasses formed from the melt, there is some evidence that the lanthanide ions substitute for network modifier ions such as alkali metals. However, the highly controlled chemical vapour deposition (MCVD) technique used in fibre fabrication keeps the concentration of these ions below the parts per billion level.

Renewed interest in this area has been stimulated by the development of lanthanide-doped fibre as an optical gain medium, most notably in the case of the erbium-doped fibre amplifier for 1.5 μm communications. Several spectroscopic studies of the Stark structure, and inhomogeneous and homogeneous broadening of the 1.5 μm erbium transition have recently been reported. Whereas earlier work on neodymium-doped fibre was particularly concerned with the temperature dependence of the homogeneous line width, interpreted in terms of coupling to dynamical modes of an ideal glass network, there is now a need to understand the way in which the composition and fabrication conditions of the fibre govern the spectroscopic characteristics of the dopant ion.

[1] Permanent address: Dept. Fisica Aplicada, C-IV, Universidad Autonoma de Madrid, 28049 Madrid, Spain.

In this work we have looked at the properties of thulium ions. Tm^{3+}, in germano- and alumino-silicate fibres. Thulium-doped fibres have been used as a laser gain medium, and show efficient broad-band operation between 1.6 and 2 μm. and also around 800 nm. Thulium is a particularly interesting ion to use as a probe of local glass structure because it has a relatively strong coupling to its surroundings, as can be seen by the particularly large inhomogeneous broadening of its optical transitions. The upper laser levels differ from those in erbium and neodymium systems in that their decay is non-radiative, making changes in phonon couplings and energies important. The level structure of Tm^{3+} shows many possibilities for cross-relaxation or energy transfer. which can be useful in the creation of up-conversion lasers [1]. The degree of cross-relaxation will be very sensitive to the distribution of Tm ions, and effects like clustering, which affect this distribution, will be of particular importance. Thus, thulium is an ideal system in which to study many of these phenomena.

2. Experimental procedures

The germano-silicate, SiO_2–GeO_2, and alumino-silicate, SiO_2–Al_2O_3, glass preforms and fibres used in this work were prepared by solution doping [2]. Thulium concentrations doped into the preform and fibre cores were estimated to be 20, 900, 6600 and 12000 ppm for the SiO_2–GeO_2 samples and 200 and 1000 ppm for the SiO_2–Al_2O_3 samples [3]. Details of the composition of preforms and fibres are given in table 1.

For the room temperature optical fibre absorption measurements presented here, the white light emission from a 12 W tungsten bulb was focused onto the entrance slit of a 1 m monochromator (Monospek 1000) and the output collimated, chopped and launched into the fibre. Light transmitted through the fibre was detected by a germanium photodiode for the 600–850 nm range or a liquid nitrogen cooled InAs photodetector (EG&G D12) for the 900–2100 nm range. The signal was pre-amplified and sent to a lock-in amplifier (Stanford Research 530), the output of

Table 1
Composition of the fibre and preform samples used in this work.

Identifier	Thulium concentration (ppm)	Core Composition
ND631	20	SiO_2–GeO_2
ND438	900	SiO_2–GeO_2
ND688	6600	SiO_2–GeO_2
ND689	12000	SiO_2–GeO_2
ND657	200	SiO_2–Al_2O_3
ND653	1000	SiO_2–Al_2O_3

which was monitored by a computer. The recorded fibre transmissions were corrected for detector and instrument response by normalising to a reference signal obtained with the detector placed immediately in front of the fibre launch optics.

Fluorescent emission spectra were measured by exciting the fibre or the preform with CW pyridine 2 dye laser emission. or using the 457 nm line of a CW argon ion laser. In both cases, the laser light was chopped using an acousto-optic modulator and focused into the core through the cleaved end of the fibre, or polished preform end. To avoid distortion of the signal due to reabsorption effects, radially emitted fluorescence was collected from the side of the core, with the first 2 cm of the sample imaged onto the slits of a 1 m monochromator. The detector used was a cooled GaAs PMT (RCA 31034-A) connected to a photon counter (Stanford SR400). Photon counting gates were set to coincide with the off cycle of the modulator. For low temperature fluorescence measurements preforms were cooled to 9 ± 0.5 K in a closed cycle cooler (CTI M22).

Lifetimes were measured using the same optics as for fluorescence studies but with the photon counter used as a boxcar averager recording the decay after the modulator switched off the exciting light. The time response of the system determined from a measurement of the scattered laser light was less than 100 ns. The decay curves were recorded by a computer and fitted to single exponential decays. An offset term was included in the decay fitting to take account of the PMT dark count.

3. Results

3.1. Absorption

The room temperature absorption spectra. from 5000 to 16000 cm^{-1}, of germano- and alumino-silicate optical fibres ND438 and ND653 (table 1) are shown in fig. 1. Energy level assignments for the thulium ion are also shown in fig. 1. Here the designation of the energy levels follows the zero spin–orbit convention [4] and as a result the 6000 cm^{-1} level has been labelled $^3H_4$, rather than the $^3F_4$. The positions of the $^1D_2$ and $^1G_4$ levels were calculated from the short wavelength limit of the fluorescence from these levels.

It can be seen from fig. 1 that despite the change of codopant from germanium to aluminium, there are no changes in the positions of
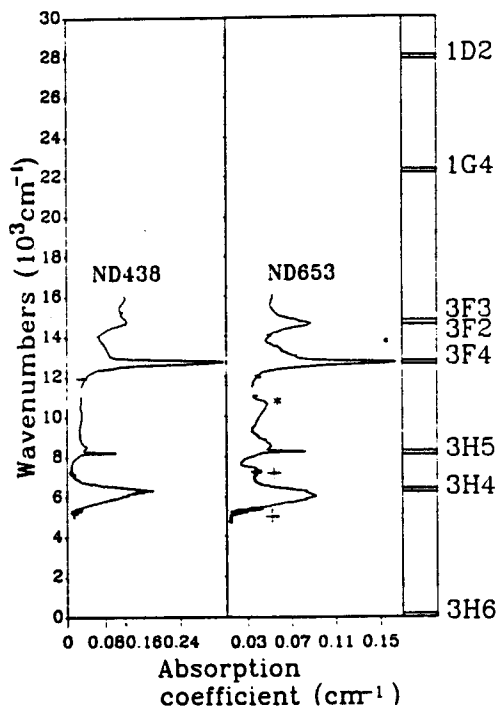

Fig. 2. Curves ND653 and ND657 show room temperature fluorescence spectra of 1000 and 200 ppm Tm^{3+}-doped SiO$_2$-Al$_2$O$_3$ glass fibre preforms. respectively. Curves ND689 and ND631 show equivalent fluorescence spectra for 12000 and 20 ppm Tm^{3+}-doped SiO$_2$-GeO$_2$ glass preforms. respectively. In all cases, samples were excited at 457 nm and side light fluorescence collected.

Fig. 1. Room temperature absorption spectra of Tm^{3+}-doped SiO$_2$-GeO$_2$ glass fibre. ND438, and Tm^{3+}-doped SiO$_2$-Al$_2$O$_3$ glass fibre. ND653. together with energy level assignments for the absorption bands. The position of the $^1D_2$ and $^1G_4$ levels was calculated from fluorescence spectra emitted from these levels. Compositions of the fibres are given in table 1.

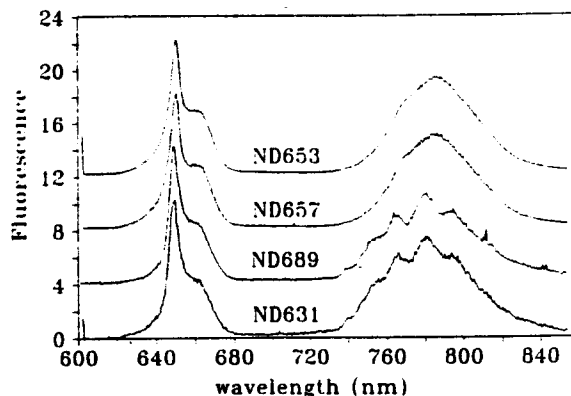the absorption peaks, although the relative magnitude of the peak heights and the high energy tails of the absorption bands are observed to change [5,6].

The feature in the absorption spectrum at 11000 cm^{-1}, marked '*' in fig. 1, is due to an artifact of the fibre geometry and has not been observed to scale with fibre length or exhibit any other properties consistent with a real absorption. The sharply peaked features at 7250 and 5250 cm^{-1}, denoted '+' in fig. 1, are due to atmospheric water absorption.

3.2. Non-resonantly excited emission

Emission spectra from 600 to 850 nm under argon ion laser excitation into the $^1G_4$ level at 457 nm were recorded for the range of germano- and alumino-silicate preforms listed in table 1. The recorded spectra for the two extremes of concentration in both types of glass are shown in fig. 2, with the 650 nm band corresponding to the $^1G_4$–$^3H_4$ transition and the 780 nm band being dominated by the $^3F_4$–$^3H_6$ transition with a small contribution from the $^1G_4$–$^3H_5$ transition.

The fluorescent spectra given in fig. 2 clearly show the strongly inhomogeneously broadened transitions frequently associated with rare earth

ions doped into glasses [7]. However. as can be seen by comparing curves ND631 and ND689 in fig. 2. no apparent changes are seen in the spectral shape of the transitions as the thulium concentration is increased 600-fold. from 20 to 12 000 ppm. Spectra recorded for the preforms ND438 and ND688, whose thulium concentrations are between these two extremes (not included in fig. 2), are also identical to those shown. This lack of variation even at high concentrations is in contrast to other results for rare earth doped silicate glasses. such as neodymium-doped SiO_2-GeO_2-P_2O_5 where changes in the spectra have been reported at dopant concentrations as low as 300 ppm [8].

When the codopant is changed from germanium to aluminium, a significant change in the spectral shape of the 780 nm transition is observed. as can clearly be seen by comparison of curves ND631 and ND689 (germanium) to curves ND657 and ND653 (aluminium) in fig. 2. This change of spectra with variation in codopant is a well known effect for other rare earths doped into silicate glasses [8]. However. further comparison of curves ND657 and ND653 in fig. 2 shows the spectra from the SiO_2-Al_2O_3 preforms again remain unchanged when the thulium concentration is increased from 200 to 1000 ppm.

Non-resonant fluorescence has also been recorded from optical fibres pulled from the pre-

Fig. 3. Comparison of the fluorescence from preform and its fibre, represented by solid and dotted lines, respectively. Comparison is shown for SiO_2-GeO_2 glass samples ND438 and ND689 (see table 1 for composition). Excitation was at 457 nm and fibre and preform spectra are normalised to the 780 nm peak.

forms listed in table 1. Overlays of the results from two separate fibre and preform pairs, both thulium-doped germano-silicates are shown in fig. 3. In comparing fibres and preforms. no differences in the position of the emission lines or changes in their width are seen. This in contrast to the 10–20% narrowing in spectral line width seen in erbium-doped silica fibres when compared to their preforms reported by Dybdal et al. [9].

The reduction in magnitude of the $^1G_4$–$^3H_5$ emission relative to $^3F_4$–$^3H_6$ emission seen in fig. 3, can be attributed to changes in the decay mechanisms of the upper states, as discussed below.

3.3. Site-selective fluorescence and fluorescence line narrowing

The $^3F_4$–$^3H_6$ emission of thulium in the germano- and alumino-silicate glasses has further been investigated under direct excitation into the $^3F_4$ level using a pyridine 2 dye laser as the excitation source and tuning this excitation across the $^3F_4$ band. This direct excitation scheme allows site selective spectroscopy, the techniques of which are reviewed by Selzer and Weber [10]. The broad-band fluorescence from 760 to 860 nm obtained by direct excitation of one germano- and one alumino-silicate sample, ND438 and ND653, respectively, cooled to 9 K and excited at a variety of wavelengths from 765–795 nm, are shown in figs. 4 and 5, respectively.

The fluorescence spectra shown in fig. 4 for the SiO_2-GeO_2 preform ND438 show three clearly resolved Stark components around 787, 803 and 815 nm, with the first component split into a doublet. For some longer excitation wavelengths, there are also at least two less clearly resolved peaks above 820 nm. although the problems of accidental degeneracy [7] make it difficult to resolve any Stark components so far from the excitation wavelength. Systematic movements in the resolved components can also be seen as the excitation wavelength is increased, indicating that the movements of individual Stark levels are correlated. This suggests the change of position of individual Stark levels within the inhomogeneous
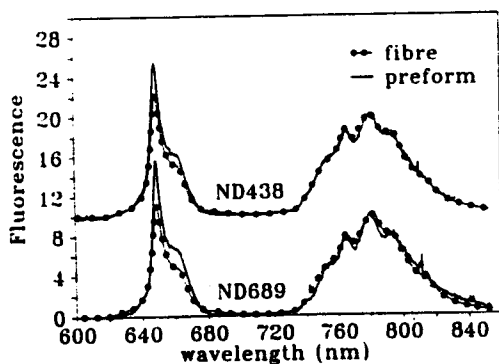
line may correspond to systematic changes of the thulium site.

Comparisons of the fluorescence from the germano-silicate preform ND438 shown in fig. 4 with the corresponding results for the alumino-silicate preform ND653 given in fig. 5 indicate that the Stark level distribution is very different in the latter glass. In the alumino-silicate spectrum, the first peak appears as a broad feature with a further two or three peaks to longer wavelength, although all features are much less distinct than in the germano-silicate preform. This is consistent with a model of the doped glass structure which suggests that the lanthanide ion will be sited near the codopant, such as germanium or aluminium, and will therefore have its local crystal field and Stark level distribution strongly influenced by the codopant [6].

Further identification of the actual site occupied by the thulium ion using this method would require identification of all ground state Stark levels not exhibiting degeneracy. However, be-
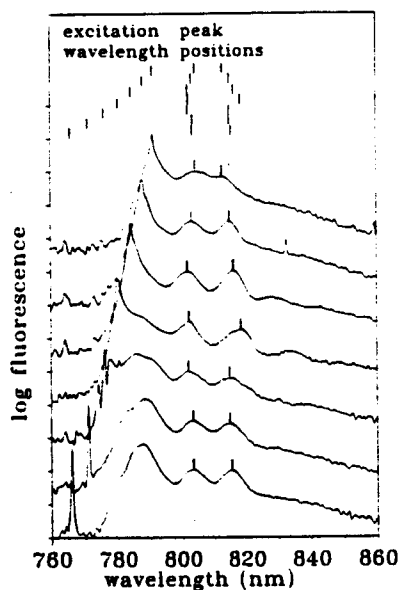

Fig. 5. Resonantly excited fluorescence from the $^3F_4$ level of Tm^{3-} in SiO_2-Al_2O_3 glass preform ND653 held at 9 K. Spectra were recorded during the off cycle of the excitation with some laser light leak through observable at the excitation wavelength. Peak positions are shown schematically above the spectra.

Fig. 4. Resonantly excited fluorescence from the $^3F_4$ level of Tm^{3+} in SiO_2-GeO_2 glass preform ND438 held at 9 K. Spectra were recorded during the off cycle of the excitation with some laser light leak through from the AO-modulator used to chop the beam observable at the excitation wavelength. Peak positions are shown schematically above the spectra.
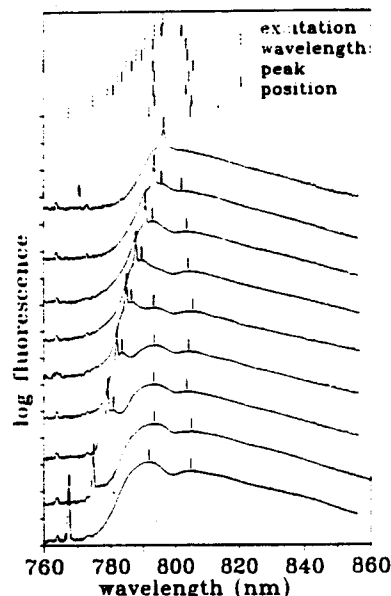
cause of the large energy spread in the Stark levels, and the difficulties apparent in resolving Stark levels far from the excitation wavelength. it is not possible to identify the 13 possible ground state levels any more explicitly.

It should be noted that the sharp spikes in figs. 4 and 5 are at the laser excitation wavelength and are due to the laser leaking through the acousto-optic modulator used to turn off the excitation beam. The laser line therefore persists in the fluorescence spectrum. However, some residual narrowed fluorescence is visible under the laser line which reflects the homogeneous width of any Stark component resonant with the laser.

Figure 6 shows much higher resolution (< 0.1 Å) spectra for alumino-silicate preform ND653 taken around the laser line in an attempt to identify the homogeneous width of the $^3F_4$ level, both with the sample at room temperature and cooled to 9 K. At room temperature no fluorescence line narrowing is observed due to very large thermal broadening [10] (the small spike apparent

in the room temperature spectrum is laser leak through). At 9 K. an additional fluorescence component is seen centred at the laser frequency, which is considerably broader than the instrumental profile. This component is taken to be the homogeneously broadened fluorescence from ions in resonance with the laser. and has a full width at half maximum of less than 10 cm^{-1}. However. the problems of deconvolving the laser line from the observed fluorescence make more precise evaluation of the homogeneous width difficult.

3.4. Decay of emission from the $^1G_4$ level

The decay of fluorescence from the $^1G_4$ energy level of the thulium ion has been studied in the full range of thulium doped germano- and alumino-silicate glasses given in table 1. For the measurement of decays, the samples were excited using argon ion laser emission at 457 nm. The lifetimes resulting from fitting single exponentials to the fluorescence decay monitored at 467 nm are presented in fig. 7(a) with lifetimes measured in preforms shown as open bars and those measured in fibres shown as solid bars.

The first characteristic to be noted from the study of the different decay times of the $^1G_4$ level shown in fig. 7(a) is a systematic shortening of the observed lifetime between any preform and its
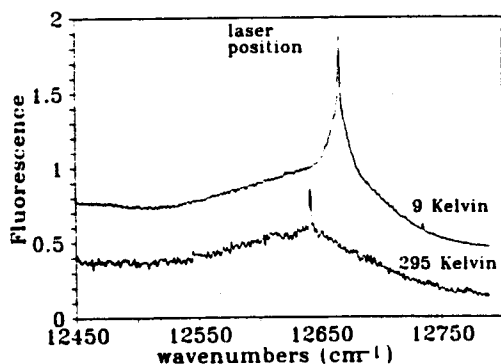

Fig. 7. Lifetimes of the $^1G_4$ level (a) and $^3F_4$ level (b) of Tm^{3+} doped into SiO$_2$–GeO$_2$ preforms and fibres (first four pairs of bars). and SiO$_2$–Al$_2$O$_3$ preform and fibre (final pair of bars). Transitions were excited at 457 nm (a) and 783 nm (b) and monitored at 464 nm (a) and 803 nm (b).

Fig. 6. Fluorescence line narrowing of the $^3F_4$ level emission of Tm^{3+} in SiO$_2$–Al$_2$O$_3$ preform ND653 at room temperature and cooled to 9 K. Excitation positions are indicated and are different for the two temperatures. Spectra were recorded during the off cycle of the excitation: however some laser leak through is observable in each spectrum.
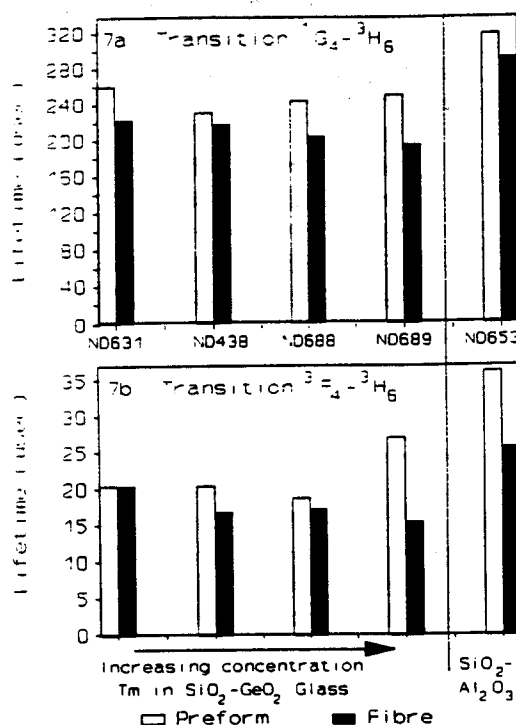
associated fibre. This shortening is always present independent of glass type or concentration and is in contrast to the results reported by Dybdal et al. [9] who observed lifetime increases between preform and fibre in erbium-doped silicate glasses. In order to verify that the observed lifetime variations are not due to the additional power density of the argon light in the fibre, which could influence some de-excitation mechanisms. decays were also recorded over two orders of magnitude of incident laser power with no variation in the results observed. We therefore consider that the shortening in lifetimes is due to the fibre pulling process, which may modify the thulium distribution or environment and so create an additional decay mechanism. Multiphonon processes can be ruled out as additional decay mechanisms since the observed lifetimes are at least five orders of magnitude shorter than the

expected multiphonon decay lifetime in silicate glasses [11], considering that the energy gap from $^1G_4$ to the immediately lower lying level, $^3F_3$, is around 7500 cm^{-1}.

Study of the first four solid bars in fig. 7(a) for the $^1G_4$ lifetime in SiO_2–GeO_2 fibres shows that the $^1G_4$ lifetime falls systematically as the concentration of thulium is increased, although the variation is less than that between preform and fibre. Such a concentration dependence suggests the additional decay mechanism is dependent on the mean separation between thulium ions. Due to this concentration dependence, we postulate that the source of the additional decay is cross-relaxation, a mechanism which has already been observed in several other thulium-doped materials [12]. This mechanism could also explain the shortening of lifetime seen in fibre drawing if the

thulium distribution is altered during the drawing process.

Further evidence of the presence of cross-relaxation in the optical fibres studied here has been provided by a comparison of the relative luminescence yield of the $^1G_4$–$^3H_5$ and $^3F_4$–$^3H_4$ transitions. Shown in fig. 3 are overlays of the preform and fibre fluorescence, solid and dotted lines, respectively, for these transitions in the samples ND438 and ND689 (table 1). In both cases, the magnitude of the 680 nm fluorescence from $^1G_4$ is seen to fall from preform to fibre (the spectra in fig. 3 are normalised to the 780 nm peak). This is the expected result if an additional non-radiative decay mechanism for the $^1G_4$ level is present in the fibre geometry, such as cross-relaxation, i.e. the radiative fluorescence from this level should be reduced in magnitude in

Table 2

Cross-relaxation schemes and the energy mismatches they involve, which are likely to depopulate the $^1G_4$ level of Tm^{3+} doped into SiO_2–GeO_2 and SiO_2–Al_2O_3 glass.

Upward transition	Downward transition				
	$^1G_4 \rightarrow ^3H_6$	$^1G_4 \rightarrow ^3H_4$	$^1G_4 \rightarrow ^3H_5$	$^1G_4 \rightarrow ^3F_4$	$^1G_4 \rightarrow ^3F_{2,3}$
$^3H_6 \rightarrow ^3H_4$					1600
$^3H_5$				800	−100
$^3F_4$			1100		
$^3F_{2,3}$		1500	−900		
$^3H_4 \rightarrow ^3F_4$				2000	200
$^3F_{2,3}$				200	
$^1D_2$	100				
$^3F_4 \rightarrow ^1D_2$		700			
$^1G_4 \rightarrow ^1D_2$					1900
	$^3F_4 \rightarrow ^3H_6$	$^3F_4 \rightarrow ^3H_4$	$^3F_4 \rightarrow ^3H_5$		
$^3H_6 \rightarrow ^1G_4$		700			
$^3H_4 \rightarrow ^3H_5$			900		
$^3F_4 \rightarrow ^3F_{2,3}$			1600		
$^1G_4$	2100				
$^1G_4 \rightarrow ^1D_2$		800			
	$^3H_4 \rightarrow ^3H_6$				
$^3H_4 \rightarrow ^3H_5$	2100				
$^1G_4 \rightarrow ^1D_2$	−600				

The mismatch energies are given in cm^{-1} and were calculated from absorption data given in fig 1. A positive entry in the table indicates the amount of energy emitted during the particular cross-relaxation scheme and is the energy required to be absorbed by the glass. Only energy mismatches between −1000 and 2500 cm^{-1} are shown; however it should be noted that, due to the very large inhomogeneous line widths observed for thulium in these glasses, fluctuations in excess of ±750 cm^{-1} are present in the figures given. No significant variation in mismatch energies were observed between the SiO_2–GeO_2 and SiO_2–Al_2O_3 glasses.

comparison with other levels. Similar effects on relative luminescence indicating cross-relaxation have already been reported by Guery et al. [12] for thulium-doped fluoride glass.

Plausible cross-relaxation processes affecting Tm^{3+} energy levels beneath the $^1G_4$ multiplet are given in table 2, together with the energy mismatches they involve calculated from the absorption data given in fig. 1. As can been seen from table 2, there are several likely cross-relaxation schemes with energy mismatches close to the maximum phonon energy in silicate glasses of around 1200 cm^{-1} [13]. An exact energy match with the phonon energy is not relevant since a large variation of ± 1000 cm^{-1} is possible in the energy mismatches quoted, due to the large inhomogeneous line widths already noted for Tm^{3+} in these glasses. From table 2 it can be seen that many of the most likely cross-relaxation schemes involve an upward transition from a second ion in the ground, $^3H_6$, state. Since this second ion does not have to be excited, such cross-relaxation schemes are much more likely than any other cross-relaxation schemes involving upward transitions from ions in an excited states. It is therefore clear that several very probable mechanisms for cross-relaxation do exist and that there observation, through lifetime shortening, is not surprising.

The $^1G_4$ lifetimes for the alumino-silicate preform and fibre, ND653, shown in the final column of fig. 7(a), clearly show that the $^1G_4$ lifetime in this glass is longer than those shown in previous columns of fig. 7(a) for germano-silicate samples. It should be noted that the lifetime in $SiO_2–Al_2O_3$ glass is not only long compared with the lifetime observed in $SiO_2–GeO_2$ samples doped with similar thulium concentrations, e.g., ND438, but also long compared with the lowest doped $SiO_2–GeO_2$ preform, ND631, where any cross-relaxation mechanism is unlikely. This suggests that the change in codopant (Al for Ge) affects the radiative probability itself, this being substantially lower in the alumino-silicate glass. However, a reduction in the $^1G_4$ lifetime between the $SiO_2–Al_2O_3$ fibres and preforms similar to that seen in the $SiO_2–GeO_2$ samples is also observed, indicating that the drawing of the fibres

also affects thulium properties in aluminium codoped fibres.

3.5. Decay of emission from the $^3F_4$ and $^3H_4$ levels

The decay of the $^3F_4$ level in the thulium ion has been studied under direct excitation using the 787 nm output from a pyridine 2 dye laser as the excitation source and monitoring the fluorescence at 802 nm. The decays recorded from the $^3F_4$ level are observed to deviate from a single exponential; however, typical fall times over the first 'e' fold of the decay are within 10% of 20 μs. Such observed decay times are an order of magnitude less than the calculated radiative lifetime of several hundreds of microseconds reported for the $^3F_4$ level in other glasses [14]. However, using the data for multiphonon decay rates in silicate glasses reported by Layne et al. [11] with the observed energy gap from the $^3F_4$ to $^3H_5$ levels of 3500 cm^{-1} gives an estimated multiphonon decay rate of tens of microseconds. One therefore deduces that, unlike to the $^1G_4$ level, the $^3F_4$ level decays predominantly by multiphonon relaxation.

The cause of the non-exponential decay of the $^3F_4$ level is the multiphonon decay mechanism exhibited by this level. We have already seen from figs. 4 and 5 that there is a large spread in the energy of the individual Stark components of the $^3H_6$ level, caused by the inhomogeneous broadening of the thulium energy levels in silicate glasses, and therefore a similar spread can be expected for the Stark components of the $^3H_5$ level. Hence the energy gap from the $^3F_4$ level to the top of the $^3H_5$ level does not have a fixed value for all the thulium ions in the sample. Even when directly exciting ions into the $^3F_4$ level and therefore selecting only ions at sites with a $^3F_4$ Stark component in common, these ions do not have to have common $^3H_5$ levels. Furthermore, it is known [15] that the multiphonon decay rate of an energy level depends exponentially on the energy gap to the next lowest level through the expression

$$k(E)_{MP} = B' \exp\left(-\alpha' \frac{E}{\hbar \omega_{ph}}\right),$$

where E is the energy gap and α', B' are constants dependent on the host and temperature, but independent of the specific electronic levels involved. This exponential dependence means that even small variations in the energy gap will strongly influence the multiphonon decay rate. In the case where an energy gap distribution, $g(E)$, exists, the intensity of fluorescence from a level. proportional to the level population, at a time, t, after turning off any excitation. can be generally expressed as

$$I(t) = I(0) \int g(E) \exp(-k(E)t)\delta E,$$

i.e. a non-exponential decay whose fall time depends on $g(E)$.

To simulate this effect of a finite energy gap distribution on the $^3F_4$ level of thulium, we have used a Gaussian approximation to the distribution $g(E)$. Conducting numerical solutions for $I(t)$, we observe decays which deviate from single exponentials and have a similar form to the experimentally measured fluorescence decays. However, we note that the decay rate obtained from fitting a single exponential decay to the numerical simulations does give a decay rate within 2% of the rate at the maximum of the simulated rate distribution. We have therefore used the results of single exponential fits to the observed decay of the $^3F_4$ level to numerically characterise this decay and hence facilitate a comparison of the different decay rates in fibres and preforms.

Figure 7(b) shows the variation of the $^3F_4$ lifetime between the different concentration fibres and preforms given in table 1. The lifetime quoted is the reciprocal of the fitted single exponential decay rate. Comparing the $^3F_4$ lifetime for germano-silicate glasses shown in the first four columns of fig. 7(b) with that for the alumino-silicate glass shown in the final column of fig. 7(b), we observe an increase in the $^3F_4$ lifetime similar to that previously noted in the $^1G_4$ decay. This is despite the $^3F_4$ fluorescence decay being predominantly governed by entirely different processes, i.e. multiphonon rather than radiative decay, and indicates the effect of the codopant on the local thulium environment. The reason for the change in the non-radiative decay rates may be either distortion of the thulium Stark levels and the effective energy gap, or changes in the vibrational characteristics of the thulium environment.

Studying the variation between the solid and open bars in fig. 7(b) for the $^3F_4$ lifetime between fibres and their preforms, we note a general shortening of the lifetime in the fibre. However, the effect of fibre drawing on the $^3F_4$ level. decaying predominantly by multiphonon mechanisms. is more variable than the effect on the $^1G_4$ decay.

The lack of any clear concentration dependence in the $^3F_4$ fibre lifetimes, shown as solid blocks in fig. 7(b), indicates that cross-relaxation has little or no influence on this level, in contrast to the observations made earlier for $^1G_4$ level. Although there is a possible cross-relaxation mechanism resulting in de-excitation of the $^3F_4$ level. namely $(^3F_4, {}^3H_6) \to (^3H_4, {}^3H_4)$, and this mechanism has been observed in thulium-doped materials [16], any cross-relaxation schemes involving the $^3F_4$ level would have to compete with the relative fast multiphonon decay already apparent for thulium in silicate glass. Hence it is not surprising that cross-relaxation effects, through thulium concentration dependence, are not observed in the $^3F_4$ fluorescence decay.

During our discussions of multiphonon processes we have noted the strong influence of the Stark level distribution of the lower lying state on the multiphonon decay processes. This is particularly relevant to the $^3H_4-{}^3H_6$ transition of thulium because of the huge spread in the $^3H_6$ Stark levels observed in the silicate glasses studied here, as was shown in figs. 4 and 5. The lifetime of the $^3H_4$ level has previously been reported by Hanna et al. [17] to be 200 μs, considerably less than the expected radiative lifetime of several milliseconds reported for this level in other glass systems [18]. If the fast decay reported by Hanna et al. is due to non-radiative relaxation of the $^3H_4$ level, then by comparison to the results for multiphonon decay in other silicate glasses [11] an energy gap of 4100 cm^{-1} is expected to the next lowest lying energy level. Such an energy gap is much smaller than the $^3H_4-{}^3H_6$ energy gap observed in the absorption

data of fig. 1, which yields a gap of approximately 5500 cm^{-1}, corresponding to a calculated lifetime of several seconds. However, one must obviously consider the reduction in the energy gap caused by the large spread in energy of the ground state Stark levels. The discrepancy between the energy gap taken from the absorption data and that required to yield the observed lifetime from multiphonon theory is 1400 cm^{-1}. This required reduction in energy gap is equivalent to the observed ground state width at 94% of maximum, measured from a fluorescence spectrum recorded with the sample held at 9 K. We can therefore confirm that the rapid decay of the $^3H_4$ level can be fully accounted for by multiphonon decay over a reduced energy gap.

3.6. Rise time of the $^3F_4$ fluorescence

The rise of the $^3F_4$ fluorescence, on turning on the exciting laser, has been measured in fibres using the same resonant excitation wavelength as used for $^3F_4$ decays. The experimental results for the 900 ppm germano-silicate fibre are shown as the discrete points in fig. 8. It was observed that the $^3F_4$ fluorescence passed through a maximum on the way to equilibrium, as can be seen on fig. 8. This behaviour is due to significant ground state depletion caused by the high pump rates
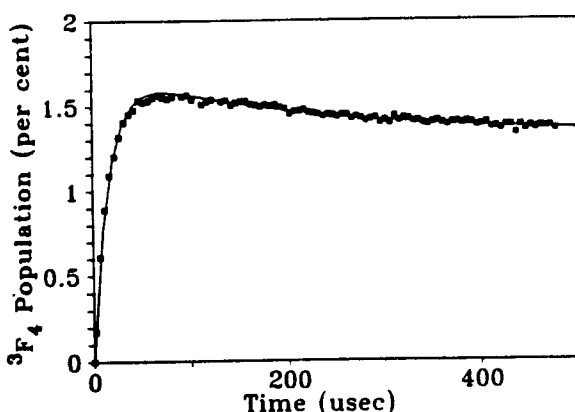

Fig. 8. Rise of fluorescence from the $^3F_4$ level in Tm^{3+} excited at 783 nm and monitored at 803 nm. The solid line is a fit to the experimental points from the solutions to a set of three-level rate equations involving the $^3F_4$, $^3H_4$ and $^3H_6$ levels.

achieved in the fibre geometry and accumulation of excited ions in the $^3H_4$ level.

To model the rise time behaviour, we constructed numerical solutions to the rate equations connecting the ground $^3H_6$ level, population N_0, the $^3F_4$ level, population N_2, and the $^3H_4$ level, population N_1. Although decay from $^3F_4$ is to $^3H_5$, any $^3H_5$ population will very rapidly relax to the $^3H_4$ level in a time scale short in comparison to the other lifetimes involved, so the presence of the $^3H_5$ level can therefore be ignored for modelling purposes. All levels higher than $^3F_4$ were taken to have a negligible effect in this simulation of $^3F_4$ excitation. One further simplification was to presume the branching ratio from the $^3F_4$ level is 100% to $^3H_5$ – this is obviously untrue as luminescence is seen from $^3F_4$, but this assumption does not change the results significantly. The rate equations therefore appear thus:

$$N_0 = -N_0 \omega_p + N_1 \omega_1,$$

$$N_1 = -N_1 \omega_1 + N_2 \omega_2,$$

$$N_2 = -N_2 \omega_2 + N_0 \omega_p,$$

with the additional condition $N_0 + N_1 + N_2 = N_T$, the total population. The only free variables in this analysis are the pump rate, ω_p, and the total population; all the other decay rates are known from experiment to be $\omega_1^{-1} = 250$ μs and $\omega_2^{-1} = 20$ μs. The solid line in fig. 8 shows the population in the $^3F_4$ level, which should be proportional to the luminescence from this level. It can be seen that the simple three-level model fits very well to the experimental data given as discrete points in fig. 8. Furthermore, the numerical model clearly shows the ground state depletion seen as a maxima in the simulated population.

The ability of the three-level model to fit the experimental data with only two variable parameters, the pump rate and the total number of ions, means that this type of analysis may be used to obtain a quantitative measurement of the absorption cross-section for the $^3F_4$ transition, using the value obtained for the pump rate by fitting the rise time of the fluorescence and a knowledge of the power incident on the fibre end. This measurement has advantages over standard methods of measuring the absorption cross-section which

frequently involve absolute calibration of detection equipment, such as integrating spheres.

3.7. Non-resonant decay of $^1D_2$

Fluorescence from the $^1D_2$ level populated by up-conversion from the $^1G_4$ level excited by 457 nm light has been observed in 900 ppm germano-silicate optical fibre. This fluorescence was centred at 360 nm and its decay was measured to be strongly bi-exponential, with 9 and 125 μs components in equal proportions. Since all levels higher than $^1D_2$ are thought to have relatively short lifetimes (< 10 μs), the most likely reason for this bi-exponential decay is that the $^1D_2$ level itself has a lifetime of order 10 μs, but is filled slowly after the laser is turned off by population decaying from $^1G_4$ to $^3H_4$, and being excited either by 457 nm absorption or by cross-relaxation involving one ion de-excited from $^1G_4$ to $^3H_6$ and one being excited from $^3H_4$ to $^1D_2$.

To verify that the observed behaviour was consistent with one of these schemes, we constructed a numerical solution of the four-level rate equations, including cross-relaxation terms. Although there are several adjustable parameters in this model, it is found that strongly bi-exponential decay can be observed for cross-relaxation rates as low as 0.1% of the pump rate, with both pump rates set equal. Hence the observation of the $^1D_2$ decay under $^1G_4$ excitation is a sensitive probe of any cross-relaxation that may be occurring. This should also apply to thulium doped into hosts other than those studied here.

4. Conclusion

The redistribution of rare earth ions and other dopants on the drawing of optical fibres may be a major limitation to fibre device performance. We have presented spectroscopic evidence for an additional decay channel for the $^1G_4$ and $^3F_4$ multiplets of thulium ions doped into germano- and alumino-silicate optical fibres which is not present in their preforms. Study of the concentration dependence of the $^1G_4$ decay in optical fibres has provided additional evidence for a cross-relaxa-

tion channel present only in the fibres. The mechanism for the additional decay channel which appears on drawing the fibres may also be cross-relaxation, although this is unclear. It is not thought to be due either to multiphonon or to radiative decay processes.

Study of an observed non-exponential decay of $^3F_4$ fluorescence of thulium ions in both alumino- and germano-silicate glass preforms and fibres has shown this decay to be consistent with an extended model of multiphonon decay, taking into account the Stark level distribution of the $^3F_4$ and $^3H_5$ multiplets.

In comparing germano-silicate and alumino-silicate cored fibres and preforms, it has been found that the $^1G_4$ decay, governed predominantly by radiative processes, and the $^3F_4$ decay, dominated by multiphonon processes, are both slower in the presence of the aluminium codopant. Alumino-silicate fibre is therefore preferable as a laser host medium.

The observed rise time of the $^3F_4$ fluorescence of thulium in germano-silicate glass has also been studied and shown to be consistent with simple models, providing a novel method of determining absorption cross-sections.

Resonant studies of the $^3F_4$–$^3H_6$ transition of thulium have also been used to probe the distribution of Stark levels of the ground $^3H_6$ state in both alumino- and germano-silicate systems. We have demonstrated that the positions of $^3H_6$ Stark levels, at sites selected by narrow line width excitation, shift in a systematic way as the selecting frequency is tuned, which may indicate that individual thulium ion sites are based on distortions of a particular basic site. Further study of the $^3H_6$ level has shown that previously reported decays for the $^3H_4$ level of Tm^{3+} in germano-silicate glass are consistent with a multiphonon relaxation mechanism if the width of the $^3H_6$ ground state is taken into account.

References

[1] D.C. Nguyen, G.E. Faulkner and M. Dulick, Appl. Optics 28 (1989) 3553.

[2] J.E. Townsend, S.B. Poole and D.N. Payne, Electron. Lett. 23 (1988) 329.

[3] Calculated by J.T. Townsend following methods of S.B. Poole, D.N. Payne, R.J. Mears, M.E. Fermann and R.I. Laming, J. Light. Tech. LT4 (1986) 870.

[4] S. Hufner, Optical Spectra of Transparent Rare Earth Compounds (Academic Press, New York, 1978).

[5] K. Arai, H. Namikawa, K. Kumata, Y. Ishii, H. Tanaka and I. Iida, Jpn. J. Appl. Phys. 22 (1983) L397.

[6] K. Arai, H. Namikawa, K. Kumata, T. Honda, Y. Ishii and T. Handa, J. Appl. Phys. 59 (1986) 3430.

[7] M.J. Weber, in: Laser Excited Fluorescence Spectroscopy in Glass, eds. W.M. Yen and P.M.Selzer (Springer, New York, 1981) p. 189.

[8] J.F. Marcerou, B. Jacquier, A.M. Briancon, J.C. Gacon, H. Fervierand J. Auge, J. Lumin 45 (1990) 108.

[9] K. Dybdal, N. Bjerre, J. Engholm Pedersen and C.C. Larson, Proc. SPIE 1171 (Fiber Laser Sources and Amplifiers) (1989) 209.

[10] P.M. Selzer and M.J. Weber, in: Laser Excited Fluorescence Spectroscopy in Glass, eds. W.M. Yen and P.M. Selzer (Springer, New York, 1981) p. 113.

[11] C.B. Layne, W.H. Lowdermilk and M.J. Weber, Phys. Rev. B 16 (1977) 10.

[12] G. Guery, J.L. Adam and J. Lucas, J. Lumin. 42 (1988) 181.

[10] S.K. Sharma, D.W. Matson, J.A. Philpotts and T.L. Roush, J. Non-Cryst. Solids 68 (1984) 99.

[14] R. Reisfeld, L. Boehm and N. Spector, Chem. Phys. Lett. 49 (1977) 251.

[15] R. Reisfeld, in: Spectroscopy of Solid-State Laser-Type Materials, ed. B. DiBartolo (Plenum, London, 1987) p. 343.

[16] G. Huber, P. Mitzscherlitch, T.-Y. Fann and R.L. Byer, J. Lumin. 40 & 41 (1988) 509.

[17] D.C. Hanna, R.M. Percival, R.G. Smart and A.C. Tropper, Opt. Commun. 75 (1990) 283.

[18] R. Reisfeld, L. Boehm and N. Spector, Chem. Phys. Lett. 49 (1977) 251.